Simanjuntak *et al. Nanoscale Research Letters* (2018) 13:327
https://doi.org/10.1186/s11671-018-2743-7

Nanoscale Research Letters

NANO EXPRESS Open Access

Switching Failure Mechanism in Zinc Peroxide-Based Programmable Metallization Cell

Firman Mangasa Simanjuntak[1], Sridhar Chandrasekaran[2], Chun-Chieh Lin[1*] and Tseung-Yuen Tseng[3*]

Abstract

The impact of peroxide surface treatment on the resistive switching characteristics of zinc peroxide (ZnO_2)-based programmable metallization cell (PMC) devices is investigated. The peroxide treatment results in a ZnO hexagonal to ZnO_2 cubic phase transformation; however, an excessive treatment results in crystalline decomposition. The chemically synthesized ZnO_2 promotes the occurrence of switching behavior in Cu/ZnO_2/ZnO/ITO with much lower operation current as compared to the Cu/ZnO/ITO (control device). However, the switching stability degrades as performing the peroxide treatment for a longer time. We suggest that the microstructure of the ZnO_2 is responsible for this degradation behavior and fine tuning on ZnO_2 properties, which is necessary to achieve proper switching characteristics in ZnO_2-based PMC devices.

Keywords: Resistive switching, Programmable metallization devices, Zinc peroxide, PMC

Background

The volatile dynamic random access memory and non-volatile flash memory have been the main leading devices for data storage application in the market; however, their further development has reached their physical limits [1, 2]. Recently, programmable metallization cell (PMC), a class of resistive random access memory (RRAM), has attracted considerable interest due to its potential for the future data storage application [3–5]. A PMC device consists of a two-terminal sandwich structure which has the advantage of the high scalability and simple fabrication [3–7].

ZnO is one of the most popular materials for various electronics; due to its low cost, non-toxic, chemically stable, low synthetic temperature, and simple fabrication process [8]. Its direct band-gap of ~ 3.3 eV makes ZnO as a suitable candidate for transparent electronic devices [9–12]. However, up to now, the ZnO-based PMC devices still need to overcome many challenges which inhibit its realization. One of the main problems is that the ZnO-based PMC devices often require high operation current due to the high n-type conductivity of ZnO material [8]. PMC device having a high-resistive storage layer is compulsory to produce switching characteristics at low operation current. Several methods have been developed to alter the switching characteristics in ZnO-based PMC devices; such as, by introducing a dopant(s) [13–18], controlling the film growth [19, 20], adding a buffer or barrier layer [16, 21], inserting a nanorod layer [22, 23], and stacking with another material(s) [24, 25]. However, those approaches still require a complicated and time-consuming fabrication process.

Recently, we reported that the employment of zinc peroxide (ZnO_2) layer in PCM cell exhibits volatile and non-volatile switching characteristics [26]. A peroxide surface treatment on ZnO surface may transform ZnO hexagonal into ZnO_2 cubic phase [27–37]. The ZnO_2 phase is found to have superior resistivity; thus, it can be exploited for Schottky contact and photodiodes applications; however, the potential of ZnO_2 for switching memory, especially the switching characteristics modulation by controlling peroxide treatment is still less investigated [26, 29–38]. Therefore, a detail investigation on the impact of peroxide surface treatment on switching

* Correspondence: chunchieh@gms.ndhu.edu.tw; tseng@cc.nctu.edu.tw
[1]Department of Electrical Engineering, National Dong Hwa University, Hualien 97401, Taiwan
[3]Department of Electronics Engineering and Institute of Electronics, National Chiao Tung University, Hsinchu 30010, Taiwan
Full list of author information is available at the end of the article

Springer Open

© The Author(s). 2018 **Open Access** This article is distributed under the terms of the Creative Commons Attribution 4.0 International License (http://creativecommons.org/licenses/by/4.0/), which permits unrestricted use, distribution, and reproduction in any medium, provided you give appropriate credit to the original author(s) and the source, provide a link to the Creative Commons license, and indicate if changes were made.

characteristics is necessary for further adoption and realization of ZnO_2-based switching memory.

Methods

ZnO thin film was deposited onto a commercial ITO/glass substrate (purchased from Uni-onward Corp.). The deposited films were immersed in hydrogen peroxide (30% H_2O_2, Perkin Elmer) solution at 100 °C for 1, 3, and 9 min. Hereafter, the surface-oxidized films were rinsed and dried with DI water and an N_2 gas gun, respectively. In order to fabricate Cu/ZnO/ITO sandwich structure devices, Cu top electrodes with a diameter of 150 μm were sputtered onto the samples (patterned using a metal shadow mask). On a separated experiment, non-surface-treated film (NT) was prepared as a control sample for comparison. STx was used for denoting surface-treated samples, where x is 1, 3, and 9 representing the treatment time (minute), respectively. Crystal structure and morphology of the films were investigated using a transmission electron microscopy (TEM, JEOL 2100FX). A semiconductor device analyzer (B1500, Agilent Tech. Inc.) was used to study the electrical characteristics.

Results and Discussion

TEM analysis was conducted to investigate the effect of peroxide treatment on the structural and morphology of the films. Figure 1a shows the cross-sectional image of ZnO film (NT) grown on ITO substrate. It is found that the growth orientation of the film is perpendicular to the substrate as shown in the high-resolution (HR) TEM image in Fig. 1b.The crystal structure of the film was investigated by analyzing the fast Fourier transform (FFT) micrograph of Fig. 1b, as depicted in Fig. 1c. The crystal structure of the ZnO film is hexagonal wurtzite structure (match with JCPDS#36-1451). The structure and morphology of the surface of the ZnO film are altered after peroxide treatment for 1 min (ST1), as shown in Fig. 1d. It can be seen that the treatment leads to a formation of a double layer. The preferred (002) orientation is diminished in the upper layer, as shown in Fig. 1e; which indicates that phase transformation is occurred due to the peroxide treatment. Figure 1f shows spot pattern analysis of FFT micrograph of (e). The upper layer is found to be polycrystalline cubic pyrite structure ZnO_2 (match with JCPDS#77-2414). It is confirmed that peroxide treatment induces hexagonal-to-cubic (h-to-c) phase transformation; this phenomenon corroborates with the previous

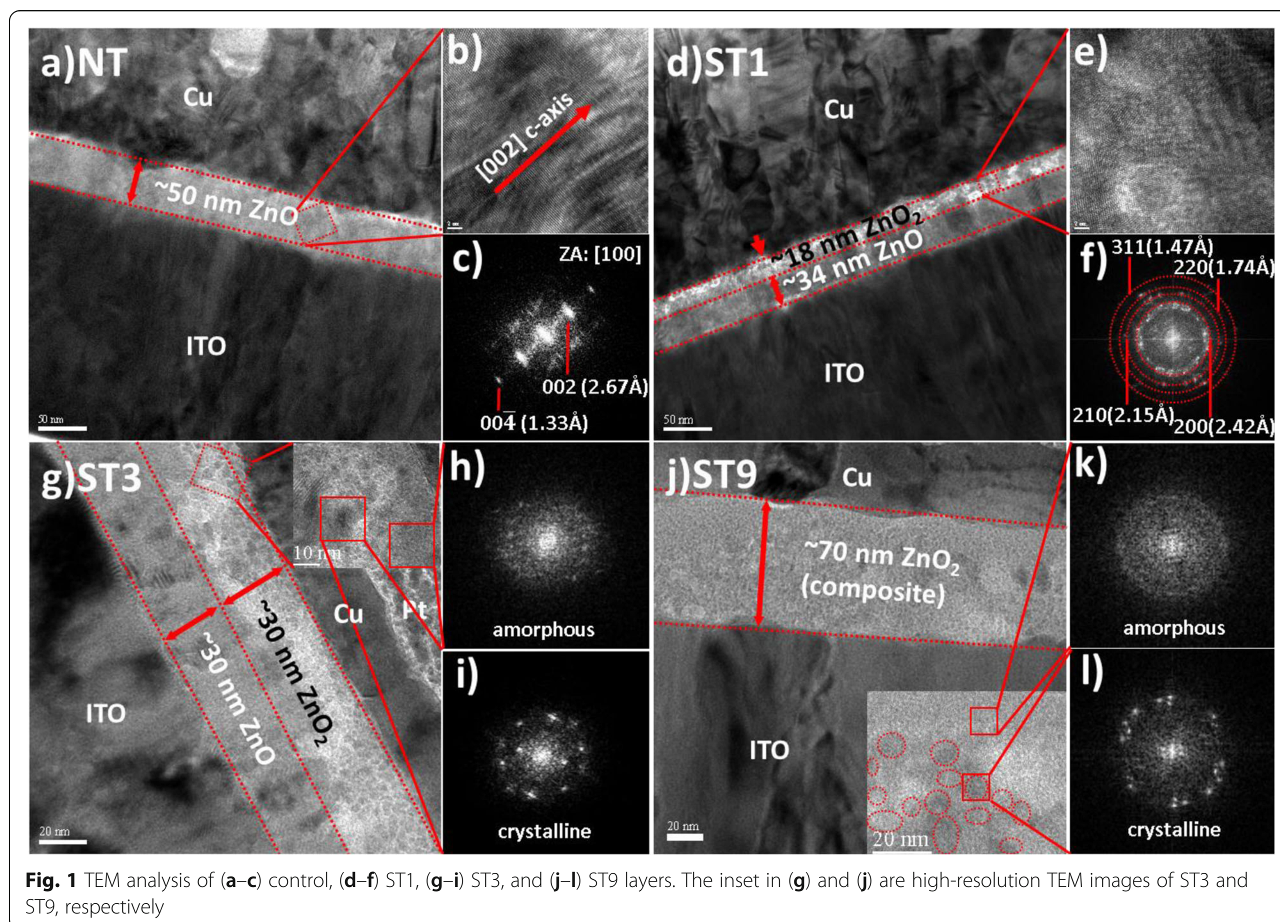

Fig. 1 TEM analysis of (**a**–**c**) control, (**d**–**f**) ST1, (**g**–**i**) ST3, and (**j**–**l**) ST9 layers. The inset in (**g**) and (**j**) are high-resolution TEM images of ST3 and ST9, respectively

literature [27, 28]. A peroxide treatment for 3 min (ST3) may lead to further oxidation into the deeper region, as depicted in Fig. 1g. The transformed region increases the total thickness of the resistive layer. The inset in Fig. 1g shows the HRTEM image of the transformed region. The FFT micrograph analysis shows that some small area has been transformed into the amorphous phase, as depicted in Fig. 1h and i. As the treatment time increases to 9 min (ST9), the phase transformation occurred in the whole region of the resistive layer, as shown in Fig. 1j. Consequently, the resistive layer consists of a single layer structure with an increased thickness of 70 nm. The inset in Fig. 1j shows the HRTEM image of the resistive layer. It can be observed that the resistive layer consists of a random distribution of nano-sized crystalline ZnO_2 particles in the amorphous matrix, as confirmed by FFT micrographs analysis shown in Fig. 1k and l. This suggests that an extended peroxide treatment may lead to a crystalline decomposition. We suppose that the excessive oxygen radicals diffused into the crystalline material may destruct its crystal structure, thus transformed into the amorphous phase [28, 39]. The electrical measurement was carried out in order to evaluate the influence of the peroxide treatment on the resistive switching characteristics.

Figure 2a shows the cross-sectional TEM image of the fabricated control (NT) device. The thickness of the top electrode (Cu), resistive layer, and bottom electrode (ITO) is approximately 400, 50, and 265 nm, respectively. ITO bottom electrode was intentionally chosen due to the ZnO/ITO ohmic contact behavior [28, 36]; thus, the switching characteristics solely rely on the resistivity of the switching layer. The schematics of the device structure and measurement setup are depicted in

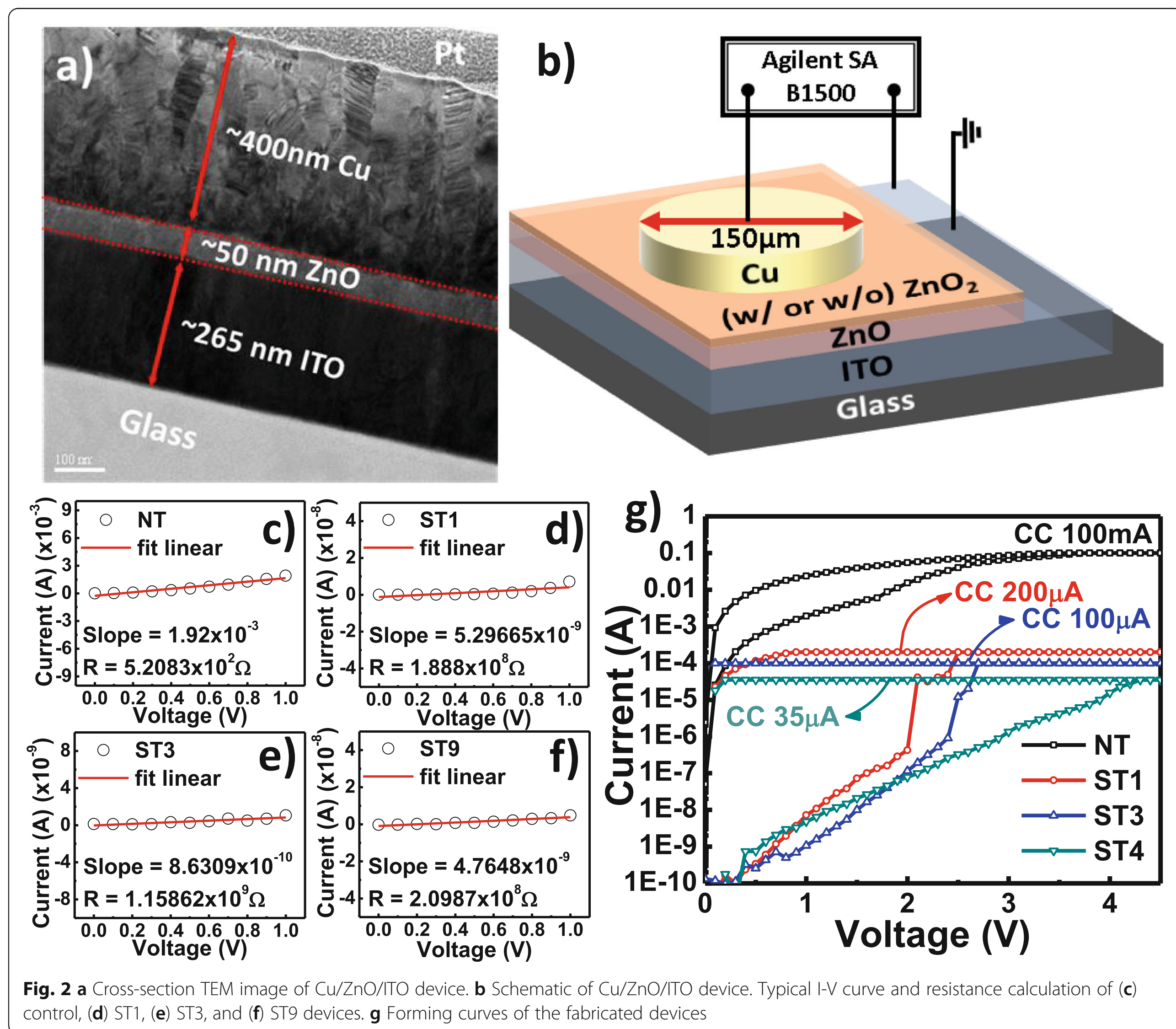

Fig. 2 **a** Cross-section TEM image of Cu/ZnO/ITO device. **b** Schematic of Cu/ZnO/ITO device. Typical I-V curve and resistance calculation of (**c**) control, (**d**) ST1, (**e**) ST3, and (**f**) ST9 devices. **g** Forming curves of the fabricated devices

Fig. 2b. The bias voltage is applied to the top electrode while the bottom electrode is ground. It is reported that the ZnO_2 possesses a very high resistivity, due to the annihilation of intrinsic donor defects and formation of acceptor defects during peroxide treatment [28–30, 32, 35, 37]. A low-voltage sweep test is conducted to calculate the resistance of the pristine devices, as shown in Fig. 2c–f. It is found that the devices made with ZnO_2 layer exhibit an increased pristine resistance, for up to 6 to 7 order of magnitude as compared to the device without the ZnO_2 layer (control device). An excessive peroxide treatment (9 min) resulted in a slight decrease in resistance of the ST9 device (Fig. 2f). Previous studies suggest that the decrease in resistance after an excessive peroxide treatment is probably due to microstructural damage such as partial etched and surface roughing [35, 37]. However, such surface damage was not observed in our TEM analysis. Nevertheless, the formation of the amorphous ZnO_2 structure occurred at the Cu/ZnO_2 interfacial region after 3 min of peroxide treatment; the crystalline-to-amorphous phase transformation starts from the surface region of the ZnO_2 film (ST3; Fig. 1g–i). We believe that the resistivity of an amorphous ZnO_2 is lesser than that of the crystalline ZnO_2. Since the ZnO_2 structure of the ST3 is mainly crystalline, therefore, the resistivity remains high (Fig. 2e). Conversely, the crystalline-to-amorphous phase transformation occurred in almost all regions of the ST9 film (Fig. 1j–l); thus, it leads to a slight decrease in resistivity (Fig. 2f). It is suggested that the number of grain boundaries has more significant role than the thickness parameter in determining the resistivity of ZnO film; higher number of the grain boundaries resulted in lower leakage current [40]. Therefore, we assume that the mechanism of the decreasing resistance phenomenon in the amorphous ZnO_2 may be similar to the ZnO case which the decreasing number of grain boundaries decreases the resistivity. Nonetheless, a detailed study on the electrical properties of the ZnO_2 material is an interesting topic that should be explored in the future.

The increase of pristine resistance is beneficial to activate the switching characteristics at lower current compliance (CC) as well as to reduce the operation current of the device. The activation of the switching characteristics is needed to change the pristine state into the low-resistance state (LRS), called as forming. Figure 2g shows the forming process of the fabricated devices. It is shown that the control device requires a very high CC of 100 mA for the forming process; conversely, ST1, ST3, and ST9 devices only require 200, 100, and 35 μA, respectively. It is found that the forming voltage of the devices made with a longer peroxide treatment tends to increase due to the increase in the total thickness of the resistive layer.

Figure 3 shows the I–V curves and endurance characteristics of the fabricated devices. All devices exhibit analog counter-clockwise bipolar switching, as shown in Fig. 3a–d. After the forming process, the devices can be switched to the high-resistance stance (HRS) by sweeping the negative voltage bias, called as reset. The reset voltage (Vreset) of all devices is − 2 V. Hereafter, the devices can be switched back to the LRS by sweeping the positive voltage (Vset) bias called as set. The statistical dispersion of Vset may elucidate the relationship between the switching parameter and the switching behavior; [11] thus, a cumulative probability is plotted as shown in Fig. 3e. It is found that the coefficient of variation (standard deviation (σ)/mean (μ)) tends to increase as the time of peroxide treatment increases, as shown in the inset of Fig. 3e. This indicates that the peroxide treatment modulates the switching parameter due to the modification of the shape or size of the conducting bridge [4, 41]. In order to evaluate the device reliability, an endurance test was conducted, and the result is

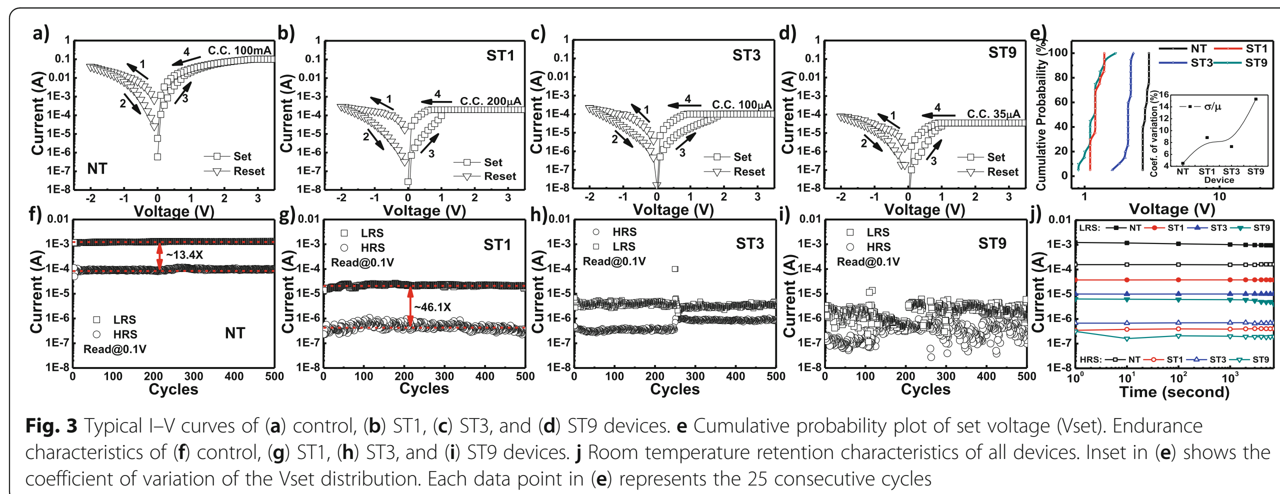

Fig. 3 Typical I–V curves of (**a**) control, (**b**) ST1, (**c**) ST3, and (**d**) ST9 devices. **e** Cumulative probability plot of set voltage (Vset). Endurance characteristics of (**f**) control, (**g**) ST1, (**h**) ST3, and (**i**) ST9 devices. **j** Room temperature retention characteristics of all devices. Inset in (**e**) shows the coefficient of variation of the Vset distribution. Each data point in (**e**) represents the 25 consecutive cycles

shown in Fig. 3f–i. The control device exhibits very stable switching with ON/OFF ratio (memory window) of approximately 13 times during endurance test, as shown in Fig. 3f. Even though the control device shows good uniformity and sufficient memory window [42], however, the operation current (100 mA) is too high; which is not suitable for low power application [43]. The switching characteristics are enhanced after 1 min of peroxide treatment (ST1), as shown in Fig. 3b and g. The ST1 device is able to operate at much lower operation current (with CC of 200 μA) and exhibits sufficient uniformity with an enlarged memory window of approximately 46 times. Further increase of peroxide treatment time allows the devices to operate at even lower operating current; the ST3 and ST9 devices are able to operate at CC of 100 and 35 μA, respectively, as shown in Fig. 3c

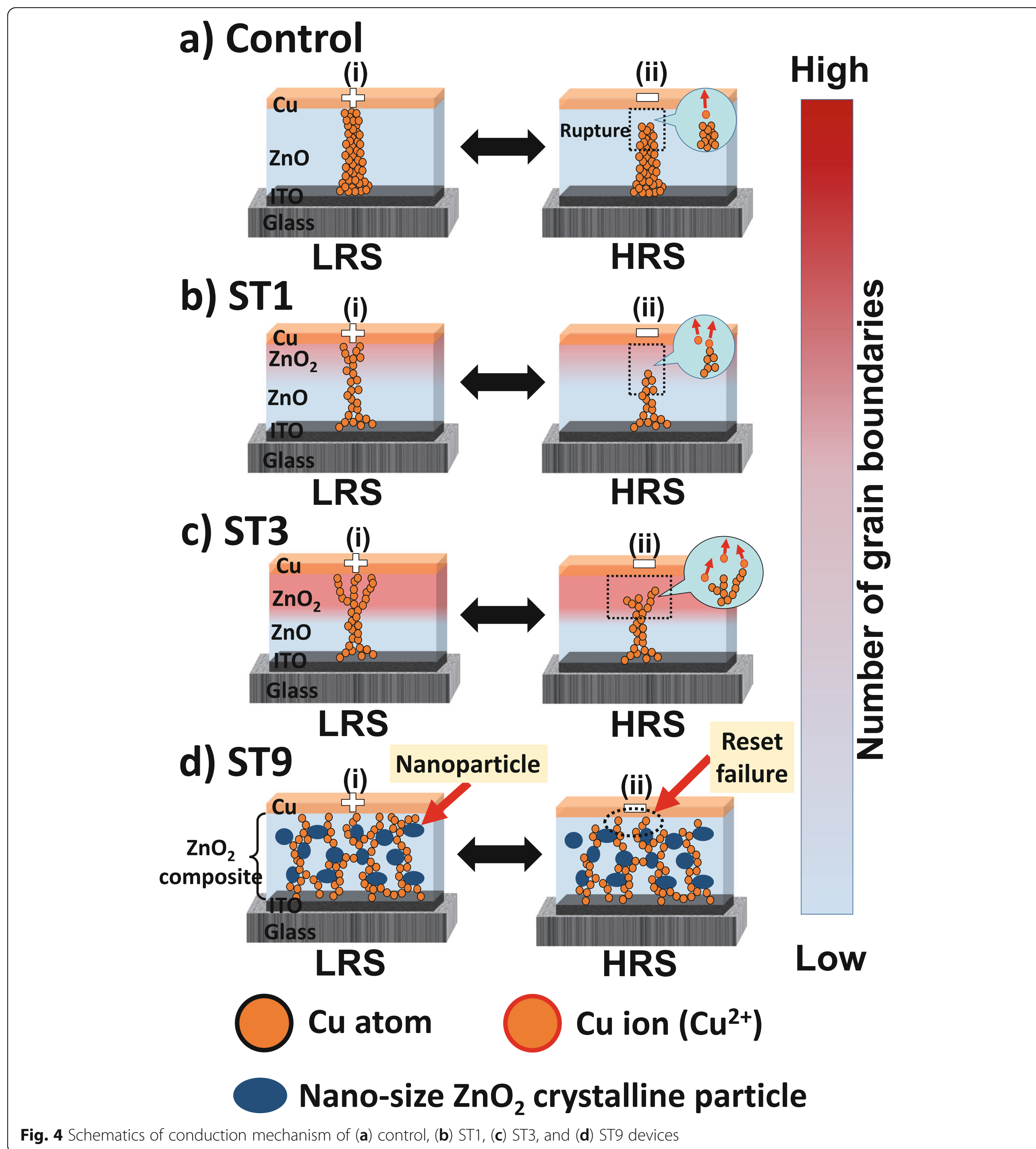

Fig. 4 Schematics of conduction mechanism of (**a**) control, (**b**) ST1, (**c**) ST3, and (**d**) ST9 devices

and d. Note that the employment of higher CC for ST3 and ST9 may result in device breakdown. Despite both ST3 and ST9 devices operate at much lower current as compared to ST1, the switching uniformity degrades as the time of peroxide treatment increases, as depicted in Fig. 3h and i. Nevertheless, all peroxide-treated devices exhibit an excellent non-volatility behavior, as shown in Fig. 3j; no significant fluctuation is observed for more than 7000 s at room temperature. Based on our previous study, the switching instability is the result of the reduction-oxidation (redox) competition between the multi- and branch conducting bridges [10, 12, 41]. We believe that the formation of the non-confined bridges is significantly controlled by the microstructure of the resistive layer.

Figure 4a–d shows the schematics of the conduction mechanism of the control device, ST1, ST3, and ST9, respectively. During forming and set processes, the Cu metal is oxidized when a positive bias is applied to the Cu top electrode (TE), and the Cu ions are attracted to the ITO bottom electrode (BE) in order to reduce to the metallic state [8]. This process results in the formation of a conducting bridge that grows from BE to the TE; consequently, the electron can easily flow from cathode to anode and resulted in the LRS (Fig. 4a (i)). Hereafter, the employment of a negative bias to the TE during reset process results in the re-ionization of Cu conducting bridge, and the Cu ions drift back to the TE; hence, the conducting bridge is ruptured, and HRS is achieved (Fig. 4a(ii)). Since the Cu ions tend to drift along the grain boundaries under an electric field [22], therefore, the perpendicular grain orientation of the ZnO resistive layer of the control device (Fig. 1b) helps the formation and rupture of a confined bridge [8]. A confined bridge is beneficial for ensuring that the formation and rupture of the conducting bridge occur at the same region; thus, high-switching uniformity is exhibited in the control device (Fig. 3f). However, the employment of high CC (100 mA) results in the formation of a large conducting bridge and high-current operation. On the other hand, the switching stability for parts of ST1 and ST3 devices degrades (Fig. 3g and h) due to the development of irregular grains (results in higher number of grain boundaries) (Fig. 1e and g). The random microstructure of the ZnO_2 layer promotes the formation of multi- or branch bridges at the respective region. Since the major area in the ST1-resistive layer is highly perpendicular to ZnO film, therefore, the formation of multi- or branch bridges can be limited (Fig. 4b(i)). Consequently, the degradation of the switching stability is minor, and good endurance performance without any intermediate state (data error) is exhibited (Fig. 4b (ii)). Conversely, a significant area of the randomly oriented ZnO_2 in the resistive layer of the ST3 device dictates the shape of the conducting bridge and results in the formation of multi- or branch bridges (Fig. 4c (i)). Hence, the formation and rupture may not occur in the same region and leads to a more serious switching instability (Fig. 4c (ii)). For the ST9 case, even though the switching layer has a low number of grain boundaries due to the crystalline-to-amorphous phase transformation, however, the random distribution of the crystalline nanoparticles leads to a severe structure irregularity. Note that since the nanoparticles are in the form of oxide, thus, no enhancement of high electric field around the particle to promote the confinement of the conducting bridge like metal inclusion does [44, 45]. Consequently, the Cu ions drifted randomly, and branched-bridge across the resistive layer is formed during forming and set processes (Fig. 4d (i)). Hereafter, the formation and rupture processes cannot be controlled at the same branch (or region) and results in the set and reset failures (Fig. 4d (ii)); thus, a severe switching instability is exhibited (Fig. 3i).

Conclusion

In summary, a switching failure mechanism in ZnO_2--based PMC devices has been proposed. The peroxide treatment promotes the formation of conducting bridge at much lower current compliance due to the high-resistivity of the switching layer. The resistance value of pristine surface-treated device can be increased up to 5 to 6 order of magnitudes. However, an excessive peroxide treatment leads to an increase structural irregularity in the switching layer; thus degrading the switching stability. This suggests that, in fact, the peroxide treatment is a useful method for obtaining low-power PMC devices; however, careful tuning of peroxide treatment is necessary to achieve good switching characteristics. The potential of this technique includes a simple fabrication process flow, scaling down the RRAM structures, and decreasing operation current/ power consumption of RRAM devices. Our simple method can be easily adopted (or explored) for many kinds of oxide systems and can encourage the realization of RRAM devices for future non-volatile memory.

Acknowledgements
The author would like to thank the support from the Ministry of Science and Technology (MOST), Taiwan.

Funding
This work was supported by the Ministry of Science and Technology, Taiwan, under project MOST 105-2811-E-259-002 and MOST 105-2221-E-259-027.

Availability of data and materials
The datasets are available from the authors on reasonable request.

Authors' contributions
FMS carried out most of the fabrication process, measurement, and analysis as well as writing the draft of the manuscript. SC conducted top electrode patterning process. The final manuscript was modified and checked by TYT and CCL. All authors read and approved the final manuscript.

Authors' information

FMS received his Ph.D. in Materials Science and Engineering from National Chiao Tung University in 2016. He joined as a post-doctoral fellow at the Department of Electrical Engineering, National Dong Hwa University. He is currently a researcher at the World Premier International Research Centers Initiative-Advanced Institute for Materials Research, Tohoku University. He specializes in surface and interfaces analysis, solid-state material characterization, synthesis of nanostructured materials, and electronic device fabrication and design. He is serving as a reviewer for a number of international publisher including Springer, MDPI, SciencePG, etc. He received a number of awards and scholarships, such as NCTU Outstanding Students Award, MME-ITS Mawapres Award, and IEFE Dissertation Scholarships.
SC received his BE degree in Electronics and Communication Engineering from Anna University, India, and M.Tech. degree in VLSI design from SRM University, India. He is currently a Ph.D. candidate of Department of Electrical Engineering and Computer Science, National Chiao Tung University, Taiwan. He is working at the Electronic Materials Laboratory of Electronics Engineering Department of NCTU where he is responsible for the development of ZrO_2-based conducting bridge random access memory devices, under the supervision of TYT. He specializes in fabrication and characterization of resistive switching memory, synaptic memory, and surface and interfacial analysis. He received a number of awards, such as NCTU Outstanding Students Award, CTCI Scholarship Award, and 2017 TACT Bronze Award.
CCL received the Ph.D. degree in electronics engineering from the Department of Electronics Engineering and Institute of Electronics, National Chiao Tung University, Hsinchu, Taiwan in 2007. He joined National Dong Hwa University, Hualien, Taiwan in 2008. He is now a Professor in the Department of Electrical Engineering. His research interests include in developing and exploring the resistive switching memory.
TYT is now a Lifetime Chair Professor in the Department of Electronics Engineering, National Chiao Tung University. He was the Dean of the College of Engineering and Vice Chancellor of the National Taipei University of Technology. He received numerous awards, such as the Distinguished Research Award from the National Science Council, Academic Award of the Ministry of Education, National Endowed Chair Professor, and IEEE CPMT Outstanding Sustained Technical Contribution Award. He is a Fellow of IEEE and American Ceramic Society.

Competing interests

The authors declare that they have no competing interests.

Publisher's Note

Springer Nature remains neutral with regard to jurisdictional claims in published maps and institutional affiliations.

Author details

[1]Department of Electrical Engineering, National Dong Hwa University, Hualien 97401, Taiwan. [2]Department of Electrical Engineering and Computer Science, National Chiao Tung University, Hsinchu 30010, Taiwan. [3]Department of Electronics Engineering and Institute of Electronics, National Chiao Tung University, Hsinchu 30010, Taiwan.

Received: 19 March 2018 Accepted: 4 October 2018
Published online: 19 October 2018

References

1. Tseng TY, Sze SM. Nonvolatile memories materials, devices and applications, Vol. 1. American Scientific Publishers, CA; 2012.
2. Panda D, Simanjuntak FM, Tseng T-Y (2016) Temperature induced complementary switching in titanium oxide resistive random access memory. AIP Adv 6:075314. https://doi.org/10.1063/1.4959799
3. Valov I, Waser R, Jameson JR, Kozicki MN (2011) Electrochemical metallization memories--fundamentals, applications, prospects. Nanotechnology 22:254003. https://doi.org/10.1088/0957-4484/22/28/289502
4. Chandrasekaran S, Simanjuntak FM, Tseng T (2018) Controlled resistive switching characteristics of ZrO 2-based electrochemical metallization memory devices by modifying the thickness of the metal barrier layer. Jpn J Appl Phys 57:04FE10. https://doi.org/10.7567/JJAP.57.04FE10
5. Chandrasekaran S, Simanjuntak FM, Aluguri R, Tseng T (2018) The impact of TiW barrier layer thickness dependent transition from electro-chemical metallization memory to valence change memory in ZrO 2 -based resistive switching random access memory devices. Thin Solid Films 660:777–781. https://doi.org/10.1016/j.tsf.2018.03.065
6. Yang JJ, Strukov DB, Stewart DR (2012) Memristive devices for computing. Nat Nanotechnol 8:13–24. https://doi.org/10.1038/nnano.2012.240
7. Aluguri R, Kumar D, Simanjuntak FM, Tseng T-Y (2017) One bipolar transistor selector - one resistive random access memory device for cross bar memory array. AIP Adv 7:095118. https://doi.org/10.1063/1.4994948
8. Simanjuntak FM, Panda D, Wei K, Tseng T (2016) Status and prospects of ZnO-based resistive switching memory devices. Nanoscale Res Lett 11:368. https://doi.org/10.1186/s11671-016-1570-y
9. Özgür Ü, Alivov YI, Liu C, Teke A, Reshchikov MA, Doğan S, Avrutin V, Cho S-J, Morkoç H (2005) A comprehensive review of ZnO materials and devices. J Appl Phys 98:041301. https://doi.org/10.1063/1.1992666
10. Simanjuntak FM, Panda D, Tsai T-L, Lin C-A, Wei K-H, Tseng T-Y (2015) Enhanced switching uniformity in AZO/ZnO 1−x /ITO transparent resistive memory devices by bipolar double forming. Appl Phys Lett 107:033505. https://doi.org/10.1063/1.4927284
11. Simanjuntak FM, Panda D, Tsai T-L, Lin C-A, Wei K-H, Tseng T-Y (2015) Enhancing the memory window of AZO/ZnO/ITO transparent resistive switching devices by modulating the oxygen vacancy concentration of the top electrode. J Mater Sci 50:6961–6969. https://doi.org/10.1007/s10853-015-9247-y
12. Simanjuntak FM, Prasad OK, Panda D, Lin C-A, Tsai T-L, Wei K-H, Tseng T-Y (2016) Impacts of co doping on ZnO transparent switching memory device characteristics. Appl Phys Lett 108:183506. https://doi.org/10.1063/1.4948598
13. Zhuge F, Peng S, He C, Zhu X, Chen X, Liu Y, Li R-W (2011) Improvement of resistive switching in Cu/ZnO/Pt sandwiches by weakening the randomicity of the formation/rupture of Cu filaments. Nanotechnology 22:275204. https://doi.org/10.1088/0957-4484/22/27/275204
14. Chao Yang Y, Pan F, Zeng F (2010) Bipolar resistance switching in high-performance Cu/ZnO:Mn/Pt nonvolatile memories: active region and influence of joule heating. New J Phys 12:023008. https://doi.org/10.1088/1367-2630/12/2/023008
15. Yang YC, Pan F, Liu Q, Liu M, Zeng F (2009) Fully room-temperature-fabricated nonvolatile resistive memory for ultrafast and high-density memory application. Nano Lett 9:1636–1643. https://doi.org/10.1021/nl900006g
16. Wei LL, Wang J, Chen YS, Shang DS, Sun ZG, Shen BG, Sun JR (2012) Pulse-induced alternation from bipolar resistive switching to unipolar resistive switching in the Ag/AgO x /Mg 0.2 Zn 0.8 O/Pt device. J Phys D Appl Phys 45:425303. https://doi.org/10.1088/0022-3727/45/42/425303
17. Shi L, Shang D-S, Sun J-R, Shen B-G (2010) Flexible resistance memory devices based on Cu/ZnO:Mg/ITO structure. Phys status solidi - Rapid Res Lett 4:344–346. https://doi.org/10.1002/pssr.201004364
18. Hu W, Chen X, Wu G, Lin Y, Qin N, Bao D (2012) Bipolar and tri-state unipolar resistive switching behaviors in Ag/ZnFe2O4/Pt memory devices. Appl Phys Lett 101:63501. https://doi.org/10.1063/1.4744950
19. Zoolfakar AS, Ab Kadir R, Rani RA, Balendhran S, Liu X, Kats E, Bhargava SK, Bhaskaran M, Sriram S, Zhuiykov S, O'Mullane AP, Kalantar-zadeh K (2013) Engineering electrodeposited ZnO films and their memristive switching performance. Phys Chem Chem Phys 15:10376. https://doi.org/10.1039/c3cp44451a
20. Huang Y, Shen Z, Wu Y, Wang X, Zhang S, Shi X, Zeng H (2016) Amorphous ZnO based resistive random access memory. RSC Adv 6:17867–17872. https://doi.org/10.1039/C5RA22728C
21. Zhao J-W, Sun J, Huang H-Q, Liu F-J, Hu Z-F, Zhang X-Q (2012) Effects of ZnO buffer layer on GZO RRAM devices. Appl Surf Sci 258:4588–4591. https://doi.org/10.1016/j.apsusc.2012.01.034
22. Simanjuntak FM, Singh P, Chandrasekaran S, Lumbantoruan FJ, Yang C-C, Huang C-J, Lin C-C, Tseng T-Y (2017) Role of nanorods insertion layer in ZnO-based electrochemical metallization memory cell. Semicond Sci Technol 32:124003. https://doi.org/10.1088/1361-6641/aa9598
23. Singh P, Simanjuntak FM, Kumar A, Tseng T (2018) Resistive switching behavior of Ga doped ZnO-nanorods film conductive bridge random access memory. Thin Solid Films 660:828–833. https://doi.org/10.1016/j.tsf.2018.03.027
24. Zhu Y, Li M, Zhou H, Hu Z, Liu X, Liao H (2013) Improved bipolar resistive switching properties in CeO 2 /ZnO stacked heterostructures. Semicond Sci Technol 28:015023. https://doi.org/10.1088/0268-1242/28/1/015023
25. Yang YC, Pan F, Zeng F, Liu M (2009) Switching mechanism transition induced by annealing treatment in nonvolatile Cu/ZnO/Cu/ZnO/Pt resistive memory: from carrier trapping/detrapping to electrochemical metallization. J Appl Phys 106:123705. https://doi.org/10.1063/1.3273329
26. Simanjuntak FM, Chandrasekaran S, Pattanayak B, Lin C-C, Tseng T-Y (2017) Peroxide induced volatile and non-volatile switching behavior in ZnO-based

electrochemical metallization memory cell. Nanotechnology 28:38LT02. https://doi.org/10.1088/1361-6528/aa80b4
27. Kashiwaba Y, Abe T, Nakagawa a, Niikura I, Daibo M, Fujiwara T, Osada H (2013) Formation of a ZnO2 layer on the surface of single crystal ZnO substrates with oxygen atoms by hydrogen peroxide treatment. J Appl Phys 113:113501. https://doi.org/10.1063/1.4792941
28. Lee H-Y, Wu B-K, Chern M-Y (2014) Study on the formation of zinc peroxide on zinc oxide with hydrogen peroxide treatment using x-ray photoelectron spectroscopy (XPS). Electron Mater Lett 10:51–55. https://doi.org/10.1007/s13391-013-2244-x
29. Chang RH, Yang KC, Chen TH, Lai LW, Lee TH, Yao SL, Liu DS Surface modification on the sputtering-deposited ZnO layer for ZnO-based schottky diode. J Nanomater. https://doi.org/10.1155/2013/560542
30. Lee H, Chern M (2015) Optical properties of ITO/ZnO Schottky diode with enhanced UV Photoresponse. J Korean Phys Soc 67:1804–1808. https://doi.org/10.3938/jkps.67.1804
31. Schifano R, Monakhov EV, Grossner U, Svensson BG (2007) Electrical characteristics of palladium Schottky contacts to hydrogen peroxide treated hydrothermally grown ZnO. Appl Phys Lett 91:19–22. https://doi.org/10.1063/1.2806194
32. Kim SH, Kim HK, Seong TY (2005) Effect of hydrogen peroxide treatment on the characteristics of Pt Schottky contact on n-type ZnO. Appl Phys Lett 86:1–3. https://doi.org/10.1063/1.1862772
33. Schifano R, Monakhov EV, Svensson BG, Diplas S (2009) Surface passivation and interface reactions induced by hydrogen peroxide treatment of n-type ZnO (0001). Appl Phys Lett 94:132101. https://doi.org/10.1063/1.3106052
34. Nakamura A, Temmyo J Schottky contact on ZnO nano-columnar film with H2O2 treatment. J Appl Phys. https://doi.org/10.1063/1.3582143
35. Gu QL, Ling CC, Chen XD, Cheng CK, Ng AMC, Beling CD, Fung S, Djurišić AB, Lu LW, Brauer G, Ong HC (2007) Hydrogen peroxide treatment induced rectifying behavior of Au / n-ZnO contact. Appl Phys Lett 90:122101. https://doi.org/10.1063/1.2715025
36. Lee H-Y, Wu B-K, Chern M-Y (2013) Schottky photodiode fabricated from hydrogen-peroxide-treated ZnO nanowires. Appl Phys Express 6:054103. https://doi.org/10.7567/APEX.6.054103
37. Lee H-Y, Su C-T, Wu B-K, Xu W-L, Lin Y-J, Chern M-Y (2011) Fabrication and properties of indium tin oxide/ZnO Schottky photodiode with hydrogen peroxide treatment. Jpn J Appl Phys 50:088004. https://doi.org/10.1143/JJAP.50.088004
38. Simanjuntak FM, Pattanayak B, Lin C-C, Tseng T-Y (2017) Resistive switching characteristics of hydrogen peroxide surface oxidized ZnO-based transparent resistive memory devices. ECS Trans 77:155–160. https://doi.org/10.1149/07704.0155ecst
39. Park SP, Yoon DH, Tak YJ, Lee H, Kim HJ (2015) Highly reliable switching via phase transition using hydrogen peroxide in homogeneous and multi-layered GaZnO x -based resistive random access memory devices. Chem Commun 51:9173–9176. https://doi.org/10.1039/C4CC10209F
40. McCandless JP, Schuette ML, Leedy KD Vertical resistivity in nanocrystalline ZnO and amorphous InGaZnO. In: Teherani FH, Look DC, Rogers DJ (eds) Oxide-based Mater. Devices IX. SPIE, p 40. https://doi.org/10.1117/12.2290624.
41. Chandrasekaran S, Simanjuntak FM, Tsai T-L, Lin C-A, Tseng T-Y (2017) Effect of barrier layer on switching polarity of ZrO2-based conducting-bridge random access memory. Appl Phys Lett 111:113108. https://doi.org/10.1063/1.5003622.
42. Waser R, Dittmann R, Staikov C, Szot K (2009) Redox-based resistive switching memories nanoionic mechanisms, prospects, and challenges. Adv Mater 21:2632–2663. https://doi.org/10.1002/adma.200900375.
43. Kim MJ, Baek IG, Ha YH, Baik SJ, Kim JH, Seong DJ, Kim SJ, Kwon YH, Lim CR, Park HK, Gilmer D, Kirsch P, Jammy R, Shin YG, Choi S, Chung C (2010) Low power operating bipolar TMO ReRAM for sub 10 nm era. Int. Electron Devices Meet. IEEE:19.3.1–19.3.4. https://doi.org/10.1109/IEDM.2010.5703391.
44. Liu Q, Long S, Wang W, Tanachutiwat S, Li Y, Wang Q, Zhang M, Huo Z, Chen J, Liu M (2010) Low-power and highly uniform switching in ZrO2-based ReRAM with a Cu nanocrystal insertion layer. IEEE Electron Device Lett 31:1299–1301. https://doi.org/10.1109/LED.2010.2070832
45. Yang Y, Gao P, Li L, Pan X, Tappertzhofen S, Choi S, Waser R, Valov I, Lu WD (2014) Electrochemical dynamics of nanoscale metallic inclusions in dielectrics. Nat Commun 5:1–9. https://doi.org/10.1038/ncomms5232

Submit your manuscript to a SpringerOpen journal and benefit from:

► Convenient online submission
► Rigorous peer review
► Open access: articles freely available online
► High visibility within the field
► Retaining the copyright to your article

Submit your next manuscript at ► springeropen.com